Wideband mm-Wave Transition Between a Coupled Microstrip Line Array and SIW for High-Power Generation MMICs

Citation for the original published paper (version of record):
Roev, A., Maaskant, R., Hook, A. et al (2018). Wideband mm-Wave Transition Between a Coupled Microstrip Line Array and SIW for High-Power
Generation MMICs. IEEE Microwave and Wireless Components Letters, 28(10): 867-869.
http://dx.doi.org/10.1109/LMWC.2018.2864869

(article starts on next page)

Wideband mm-Wave Transition Between a Coupled Microstrip Line Array and SIW for High-Power Generation MMICs

Artem Roev, *Student Member, IEEE*, Rob Maaskant, *Senior Member, IEEE*, Anders Höök, and Marianna Ivashina, *Senior Member, IEEE*

***Abstract*— A compact wideband transition between an array of microstrip lines (MLs) and a single substrate integrated waveguide (SIW) is presented. The spatially distributed fundamental SIW mode is excited by an array of parallel and strongly coupled MLs. The proposed configuration is optimized by minimizing the "active" reflection coefficient at each ML port. Signals are transferred with nearly uniform power distribution across the ML ports, which facilitate an effective utilization of power amplifiers once interconnected. Measured results of the proof-of-concept demonstrator are in good agreement with simulations. The proposed configuration is capable of generating more power per footprint size relative to a single microstrip-to-SIW transition while offering a 50% bandwidth. At the same time, the compactness of the ML-to-SIW transition makes it suitable for tight integration with monolithic microwave integrated circuits and applications in wideband array antennas.**

***Index Terms*— Grid amplification, integration, mode converter, monolithic microwave integrated circuits (MMICs), parallel power combiner, quasi-optical beamforming, spatial power combining, substrate integrated waveguide (SIW).**

I. Introduction

EFFICIENT generation and transmission of high RF power are a major challenge at mm-wave frequencies, due to the increased propagation and material losses as well as output power limitations of semiconductor technologies [1]. Silicon-based technologies are not often the first choice due to their relatively low breakdown voltage, however, significant research has been put into it as they enable cost-effective highly integrated circuit solutions. The focus of this letter is on a compact wideband transition between an mm-wave integrated circuit and an antenna or waveguiding structure.

Manuscript received June 29, 2018; accepted August 6, 2018. Date of publication September 18, 2018; date of current version October 5, 2018. This work was supported by the European Unions Horizon 2020 Research and Innovation Program through the Silicon-based *Ka*-band Massive Multi-in Multi-out Antenna Systems for New Telecommunication Services (SILIKA) Project by Marie Skodowska Curie under Grant #721732. *(Corresponding author: Artem Roev.)*

A. Roev and M. Ivashina are with the Electrical Engineering Department, Chalmers University of Technology, S-41296 Gothenburg, Sweden (e-mail: roev@chalmers.se).

R. Maaskant is with the Electrical Engineering Department, Chalmers University of Technology, S-41296 Gothenburg, Sweden, and also with the Electrical Engineering Department, Eindhoven University of Technology, 5612 AZ Eindhoven, The Netherlands.

A. Höök is with the SAAB AB, 412 76 Gothenburg, Sweden.

Color versions of one or more of the figures in this paper are available online at http://ieeexplore.ieee.org.

Digital Object Identifier 10.1109/LMWC.2018.2864869

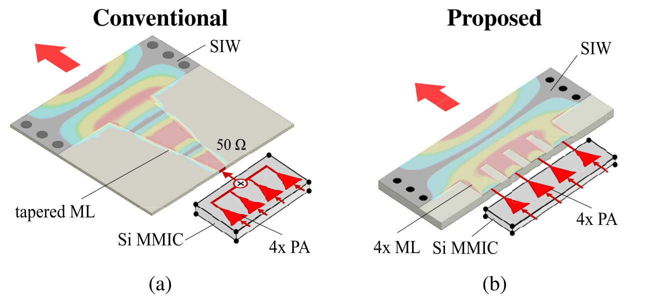

Fig. 1. (a) Classical single-channel transition interfacing an array of PAs with an SIW. (b) Proposed novel transition.

TABLE I
COMPARISON BETWEEN THE STATE-OF-THE-ART SOLUTIONS AND THE PROPOSED DESIGN

Reference	Freq, [GHz]	Bandwidth, [%]	Losses (b2b), [dB]	SIW width, [λ]
single-, TE10 [3]	25-31	12	0.15	0.50-0.62
single-, TE10 [4]	17.5-30	50	1	0.44-0.76
multi-, TE20 [6]	20-40	50	2	0.57-1.14
multi-, TE10 [this work]	22-36	48	0.3	0.51-0.84

The key design goals are: 1) wide frequency bandwidth (BW) (∼50%); 2) minimal power losses when transmitting and combining signals from power amplifiers (PAs); 3) quasi-optical power combining using grid amplification techniques, i.e., employ multiple PAs to generate high mm-wave power in the range of 15–25 dBm per antenna element. This is challenging for silicon integrated solutions particularly because the on-chip power combiner and the antenna interconnecting transition must be low loss [2]; and 4) minimal dimensions to render the transition suitable for antenna integration, specifically for arrays (with interelement spacing $<0.8\lambda$), and allow for on-chip integration at a later stage.

Fig. 1(a) exemplifies a conventional microstrip line (ML) to substrate integrated waveguide (SIW) transition [3], [4], which was used as a starting point in our design. As illustrated, the chip with multiple PAs delivers high power to the input port of the transition which is then transferred to the SIW. The critical design parameter is the effective impedance of the SIW, which in practice, is significantly lower than the typical 50-Ω interface impedance of the (PA) chip. Achieving optimal impedance match renders the transition long, and therefore lossy, especially if a wide frequency BW is required

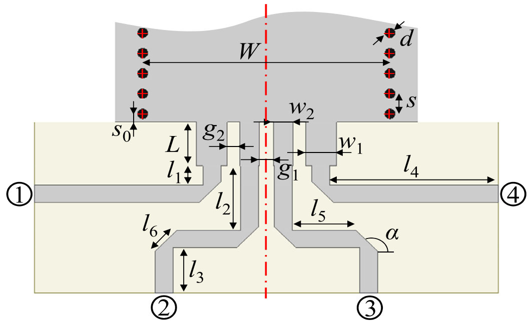

Fig. 2. Proposed DUT including routing lines to connectors.

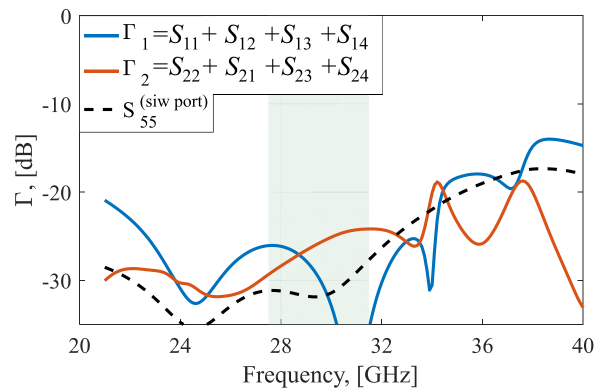

Fig. 3. Simulated active reflection coefficients of the 50-Ω microstrip ports and wave port passive reflection (dashed) of the DUT, as shown in Fig. 2. Colored region: band of interest.

(see [3], [4], and Table I). This fundamental tradeoff between BW and power losses for a single-channel transition does not exist for the recently proposed multichannel transition [5], which directly interfaces an array of PAs to an SIW via multiple spatially distributed MLs [see Fig. 1(b)]. Fig. 1 also visualizes the transfer from the ML mode(s) to the fundamental TE10 SIW mode. The MLs are closely spaced and, hence, strongly coupled, which cause mutual coupling effects to play a critical role in the proposed transition performance and its design process. Note that, this concept differs from the parallel multichannel systems used in overmoded SIWs [see [6], Table 1], where the MLs are spatially separated. This prevents tight integration with monolithic microwave integrated circuits (MMICs), and leads to a wide SIW, limiting its applications in array antennas

II. Numerical Results

The proposed transition has been designed through "active" impedance matching, a technique known from antenna array network theory. It allows the reflection coefficient of each ML mode to be analyzed in the presence of the ML array excitation and ML array mutual coupling effects, with the ultimate goal to maximize the overall power transfer to the SIW. To this end, we minimize the "active" reflection coefficients at the input ports under the condition of a matched terminated SIW output port (not excited). Assuming a uniform excitation of the ML ports, the active reflection coefficients are computed as: $\Gamma_n = \sum_{m=1}^{M} S_{nm}, n \in \{1, 2, 3, 4\}$, where S_{mn} is a scattering parameter, and $M = 4$ in the present case.

Fig. 2 shows the geometry of the transition, which was modified to allow for connectorized measurements; divergent MLs to connectors were included into device under test (DUT) to be able to mount RF connectors to the printed circuit board (PCB) and to decouple the MLs. Only a two-port calibration kit was needed to remove the effect of connectors from the measurement results. The structure in Fig. 2 employs the RT4350 laminate with thickness 0.254 mm and relative dielectric constant of $\varepsilon_r = 3.66$. The optimum design parameters leading to minimum reflections over the desired frequency band are (in millimeters): $L = 1.35$; $W = 7.33$; $d = 0.3$; $s = 0.6$; $w_1 = 0.92$; $w_2 = 0.57$; $g_1 = 0.42$; $g_2 = 0.37$; $l_1 = 0.60$; $l_2 = 2.00$; $l_3 = 1.40$; $l_4 = 5.00$; $l_5 = 1.90$; $l_6 = 0.63$; and $\alpha = 135°$. It is worth mentioning that w_1 and w_2 are not equal due to the fact that active line impedances are different between the inner and outer two coupled all excited MLs.

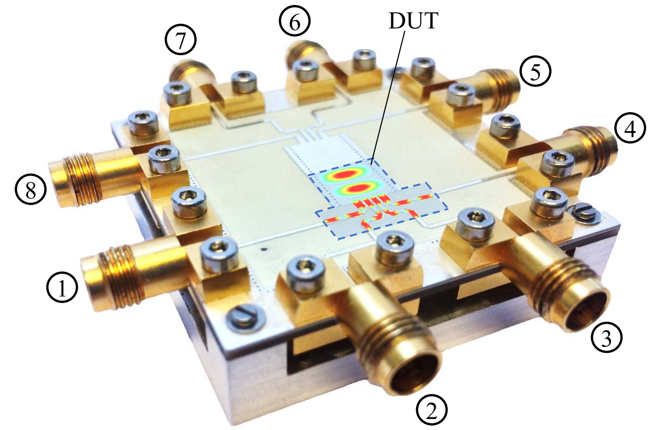

Fig. 4. DUT in a B2B configuration.

The 50-Ω simulated active and passive reflection coefficients (Γ_1,Γ_2, S_{55}^{siw}) in the desired frequency range (27.5–31.5 GHz) are shown in Fig. 3. The multichannel transition demonstrates wide BW (beyond 50% relative BW) with both $|\Gamma_1|$ and $|\Gamma_2| < -15$ dB. A sensitivity study on Γ was performed and shows that $|\Gamma|$ remains below -15 dB in the case of normal distributed phase errors of signals across the ML ports with a standard deviation $< 15°$.

III. B2B Prototype and Measurement Results

The designed prototype constitutes a passive back-to-back (B2B) structure employing four input and four output 50-Ω coaxial ports to allow for testing with a standard vector network analyzer (see Fig. 4).

The structure is built on a hybrid multilayer PCB, which is formed by stacking two dielectric material layers. The top RT4350 laminate has a substrate thickness of 0.254 mm and of $\varepsilon_r = 3.66$. The bottom hardback substrate is FR4, which makes the structure more rigid. The interior metal layers of the hybrid structure can be used in the future for routing, bias, or control lines of an active device. The PCB has the overall size of approximately 46 × 46 mm.

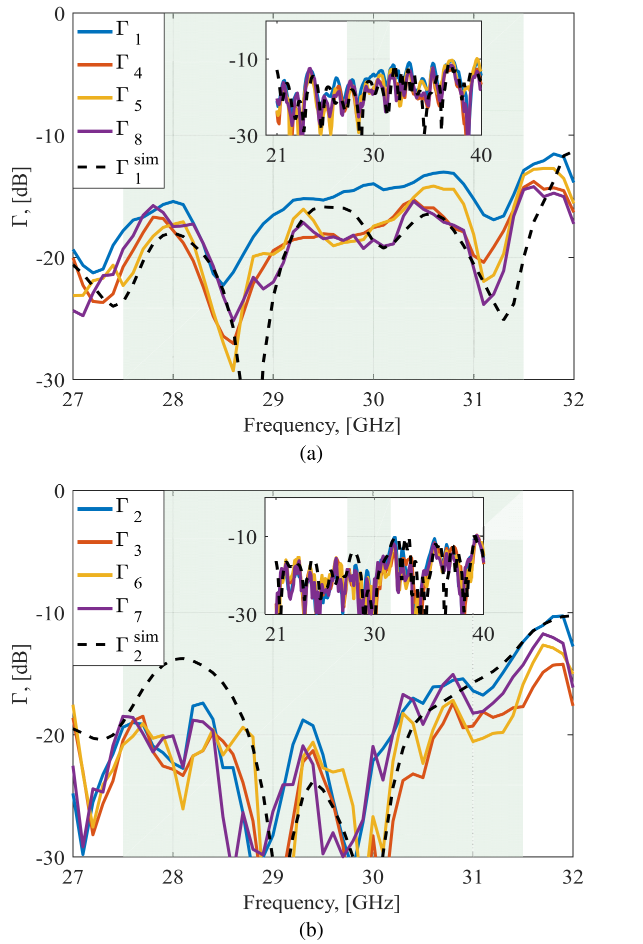

Fig. 5. Measured (solid) and simulated (dashed) active reflection coefficient of the symmetric 50-Ω microstrip ports of the prototype (including effect of connectors), as shown in Fig. 4.

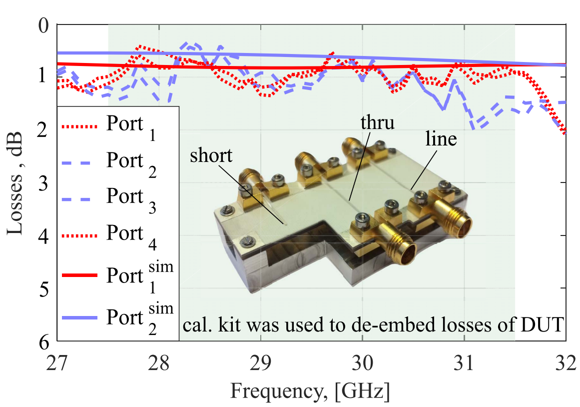

Fig. 6. Measured (dashed) and simulated (solid) losses of the proposed DUT.

The measured Γ of the symmetric 50-Ω ports is shown in Fig. 5. Curves are close to each other and in good agreement with the simulations shown by black dashed lines. Visible ripples are produced by the connector interfaces and bent microstrip transmission lines whose effects cannot be completely removed by the designed two-port thru-reflect-line calibration kit, since, in practice, ports are slightly different. However, the measured $|\Gamma_1|$ and $|\Gamma_2| < -13$ dB in the desired frequency range and < -10 dB over the whole range (20–40 GHz).

Insertion losses of the proposed DUT are shown in Fig. 6. The measured losses were deembedded using the thru standard of the designed calibration kit. Contributions of the dielectric and radiation losses have been estimated using the simulation data. At 30 GHz, the total losses of the DUT are 0.73 dB, where the contribution of the dielectric and radiation losses is 0.28 and 0.45 dB, respectively. Radiation losses are dominant and attributed to the bent MLs in the DUT. The overall expected losses of the proposed transition without routing lines are estimated less than 0.3 dB.

IV. Conclusion

A new transition for interfacing an array of parallel amplifiers to a single SIW has been optimized and examined in the context of its applications in wideband and high-efficiency array antenna transmitters. The proposed transition overcomes fundamental limitations of single-channel SIW transitions in simultaneously achieving a wide BW and low power loss, and also outperforms the state-of-the-art multichannel multimode transitions in terms of its compactness and power transfer/combining efficiency (see Table 1). The proof-of-concept experiments demonstrate a good agreement with simulated performance, where we have achieved an active impedance BW defined at −10 dB of nearly 50% (20–40 GHz) with the estimated losses less than 0.3 dB. Furthermore, a nearly uniform power distribution across the parallel ports confirms that the PAs in the array will be utilized efficiently. The concept is expected to facilitate high-power generation and efficient power transmission in the future mm-wave array antennas and MMIC designs.

References

[1] J. Edstam *et al.* (Feb. 2017). *Ericsson Technology Review: The New Microwave Backhaul Frontier*. [Online]. Available: https://www.ericsson.com/assets/local/publications/ericsson-technology-review/docs/2017/etr-beyond-100ghz.pdf

[2] K. H. An *et al.*, "Power-combining transformer techniques for fully-integrated CMOS power amplifiers," *IEEE J. Solid-State Circuits*, vol. 43, no. 5, pp. 1064–1075, May 2008.

[3] D. Deslandes and K. Wu, "Integrated microstrip and rectangular waveguide in planar form," *IEEE Microw. Wireless Compon. Lett.*, vol. 11, no. 2, pp. 68–70, Feb. 2001.

[4] F. Taringou, D. Dousset, J. Bornemann, and K. Wu, "Substrate-integrated waveguide transitions to planar transmission-line technologies," in *IEEE MTT-S Int. Microw. Symp. Dig.*, Jun. 2012, pp. 1–3.

[5] A. Roev, R. Maaskant, M. Ivashina, and A. Höök, "Wide-band spatially distributed TE10 substrate integrated waveguide transition for high-power generation at mm-wave frequencies," in *Proc. Int. Symp. Antennas Propag. (ISAP)*, Oct./Nov. 2017, pp. 1–2.

[6] A. Suntives and R. Abhari, "Design and application of multimode substrate integrated waveguides in parallel multichannel signaling systems," *IEEE Trans. Microw. Theory Techn.*, vol. 57, no. 6, pp. 1563–1571, Jun. 2009.